catalysts

MDPI

Article

Facile Synthesis of COF-Supported Reduced Pd-Based Catalyst for One-Pot Reductive Amination of Aldehydes

Jianguo Liu [1,2,*], Mingyue Zhang [1,3] and Longlong Ma [1,*]

[1] Key Laboratory of Renewable Energy, CAS, Guangdong Key Laboratory of New and Renewable Energy Research and Development, Guangzhou Institute of Energy Conversion, Chinese Academy of Sciences, Guangzhou 510640, China; zhangmy@ms.giec.ac.cn
[2] Dalian National Laboratory for Clean Energy, Dalian 116023, China
[3] University of Chinese Academy of Sciences, Beijing 100049, China
* Correspondence: liujg@ms.giec.ac.cn (J.L.); mall@ms.giec.ac.cn (L.M.)

Abstract: Dibenzylamine motifs are an important class of crucial organic compounds and are widely used in fine chemical and pharmaceutical industries. The development of the efficient, economical, and environmentally friendly synthesis of amines using transition metal-based heterogeneous catalysts remains both desirable and challenging. Herein, we prepared the covalent organic framework (COF)-supported heterogeneous reduced COF-supported Pd-based catalyst and used it for the one-pot reductive amination of aldehydes. There are both Pd metallic state and oxidated $Pd^{\sigma+}$ in the catalysts. Furthermore, in the presence of the reduced COF-supported Pd-based catalyst, many aromatic, aliphatic, and heterocyclic aldehydes with various functional groups substituted were converted to their corresponding amines products in good to excellent selectivity (up to 91%) under mild reaction conditions (70 °C, 2 h, NH_3, 20 bar H_2). This work expands the covalent organic frameworks for the material family and its support catalyst, opening up new catalytic applications in the economical, practical, and effective synthesis of secondary amines.

Keywords: COF; reduced COF-supported Pd-based catalyst; reductive amination; secondary amines

check for updates

Citation: Liu, J.; Zhang, M.; Ma, L. Facile Synthesis of COF-Supported Reduced Pd-Based Catalyst for One-Pot Reductive Amination of Aldehydes. *Catalysts* **2021**, *11*, 287. https://doi.org/10.3390/catal11020287

Academic Editor: Sergio Carrasco

Received: 2 February 2021
Accepted: 18 February 2021
Published: 22 February 2021

Publisher's Note: MDPI stays neutral with regard to jurisdictional claims in published maps and institutional affiliations.

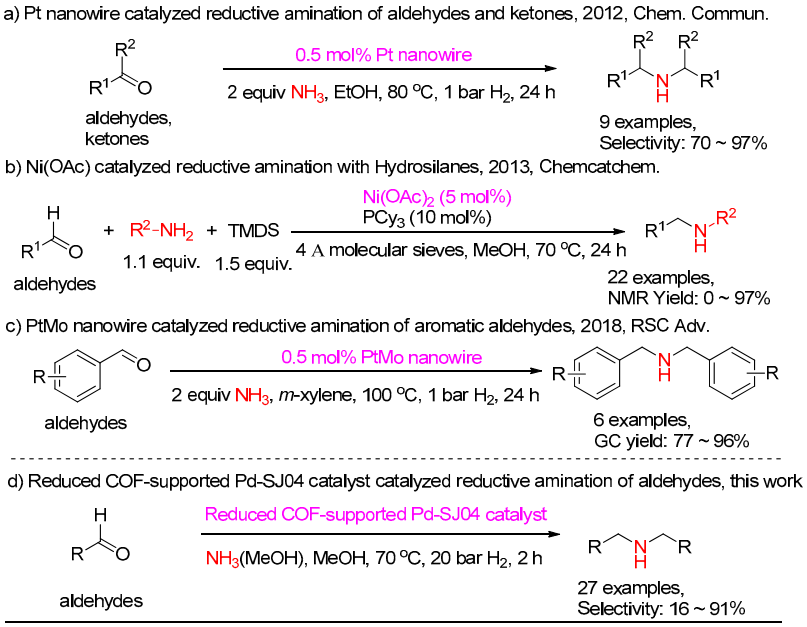
Copyright: © 2021 by the authors. Licensee MDPI, Basel, Switzerland. This article is an open access article distributed under the terms and conditions of the Creative Commons Attribution (CC BY) license (https://creativecommons.org/licenses/by/4.0/).

1. Introduction

Dibenzylamine motifs are presented as a class of crucial organic compounds with extensive applications in rubber compounds, constituting attractive intermediates for fine chemical industries, corrosion inhibitors, and drug formulations [1–7]. The development of a highly efficient selective synthesis method has attracted great attention in organic chemistry. In general, conventional methodologies for their production involve either direct base-promoted mono-N-alkylation or alkylative amination [8–10]. Although significant research efforts have proceeded, problems such as tedious workup process, poor product yield or selectivity, and large byproduct formation of wasteful salts need to be solved according to the environmental and sustainable issues. Reductive amination of carbonyl compounds using transition-metal catalyst has become a highly versatile and robust method for various transformations in the C–N bond construction due to its obvious advantages, such as mild reaction conditions, wide availability, and inexpensive reagents [4,7,10]. Moreover, the activation of H_2 and the catalytic reduction of unsaturated compounds are fundamentally promising environmentally friendly processes. However, in the reductive amination of benzaldehyde using H_2 and ammonia, for example, the controllable selective process to either 100% benzylamine or 100% dibenzylamine is very challenging. It is generally assumed that the reaction conversion and final product composition mainly rely on the catalyst metal component. In this respect, various transition metal systems, such as Raney Ni, Pd-based, Pt-based, etc., have been applied widely in reductive amination for the synthesis of amines [11–16]. Raney Ni was used widely and proved to be very suitable for the reductive amination of benzaldehyde with NH_3. However, due to

the low product selectivity, lack of safety, and harsh reaction conditions, its application in the industry was restricted. Recently, more resistant unsupported or supported noble metals showed the high reactivity and selectivity of reductive amination under milder reaction conditions. For example, Qi et al. [3] developed the selective synthesis of secondary amines through direct reductive amination of aldehydes using the unsupported Pt nanowire catalyst under mild reaction conditions (80 °C, 24 h, 2 equivalent NH_3, 1 bar H_2) (Scheme 1a). They found that the dibenzylamine (DBA) selectivity increased from 82.5 to 93.3% and dibenzylimine (DBI) selectivity decreased from 14 to 3.3% when the reaction temperature increased from 40 to 80 °C. Compared with Pt nanorods (80.3%) and nanoparticles (59.2%), the Pt nanowire catalyst exhibited excellent dibenzylamine selectivity (93.3%) in reductive amination using ammonia or ammonium acetate as the substrate. According to their time-conversion results from gas chromatography (GC), they agreed with their proposed mechanism: The reaction intermediate is dibenzylimine, which is stable and can be detected, and the reduction of dibenzylimine is the rate-determining step. Hydrogenation of imines or direct hydrogenolysis of carbinol-amines can produce benzylamine and dibenzylamine as products. However, there is generally an exit competing reaction to form benzyl alcohol via the direct hydrogenation of benzaldehyde. Surprisingly, the Pt nanowire catalyst can be easily recycled and reused up to six times without Pt leaching. Later, Zhang et al. [17] reported nickel-catalyzed reductive amination of aldehydes by hydrosilylation using an in situ-generated catalytic system from inexpensive nickel acetate and tricyclohexylphosphine (Scheme 1b). Under the optimized reaction conditions (1.1 equivalent amine, 1 equivalent aldehyde, 70 °C, 8 h, then 1.5 equivalent tetramethyldisiloxane, 70 °C, 16 h), various amines including aromatic and aliphatic amines were tested with aromatic aldehydes or aliphatic aldehydes. The corresponding secondary amines were obtained in good to excellent conversions and yields. However, secondary amine and ketones were not well-tolerated under similar reductive amination conditions. They mixed $Ni(OAc)_2$, PCy_3 and Ph_2SiH_2, and found that the mixture turned orange-red after 3.5 h at 100 °C. According to the NMR analysis, they confirmed that the complex $[\{Ni(PCy_3)\}_2(m\text{-}SiHPh_2)_2]$ was formed in situ. Since in the ^1H NMR spectrum, the main compound revealed a signal at −2.04 ppm, which is assigned for Ni(H-Si), and a signal at +45.9 ppm was also observed in the ^{31}P NMR spectrum, and this observation matched well with the previous report by Osakada et al. [18]. The first step of the catalytic cycle was confirmed to be the reduction of Ni^{II} to Ni^0 species by these spectrometric data. Recently, Lu et al. [6] prepared new worm-like PtMo nanowires through facile co-reduction of Pt and Mo precursors with H_2 (Scheme 1c). The as-prepared nanowires work effectively in the activation of H_2, following which, dibenzylamines can be successfully synthesized from the reductive amination of either benzaldehyde or benzonitriles under mild and green reaction conditions. Due to the high stability of Mo precursors against inferior reductants, Mo was observed with low content. According to the elemental mapping analysis, Pt and Mo are well-distributed throughout the interior and exterior domains. The Pt catalytic activity and stability were enhanced by the incorporation of Mo into Pt. Pt active sites were liberated when H_2 on the surface of Pt sites migrated over to the Mo species. They found that the catalyst was readily recovered, can be easily scaled up and was very active due to its composition and morphological effects in the reaction of imines into amines.

With the increasing problems concerning environmental and sustainable chemistry, many classes of transition metals like Pd, Rh, etc., -based heterogeneous catalysts had been developed and widely used. They showed excellent activities and selectivities for the product amine synthesis. As is well-known, the catalyst supports can control the active metal nanoparticles' size, distribution, surface electronic properties, which significantly affected the metal-supported catalyst's intrinsic activity and selectivity [19–23].



Scheme 1. Reported methodologies [3,6,17] and this work for the selective production of amines via various transition metals based catalytic systems.

Covalent organic frameworks (COFs) have become one important class of the most promising porous support materials since they were first reported by Cote et al. [24]. They have been extensively studied due to their fascinating features, including low density, high and regular porosity, high stability, tunable pore size, strong covalent bonds, and easy design of functional groups. Recently, COFs were applied to construct core-shell structure composite materials (graphene, carbon nanotubes, Fe_3O_4, and alumina, etc.) via heterogeneously nucleating and growing on the surface of different matrices [25–28]. The nanosized core's aggregation can be effectively impeded via the incorporation of COF merits and nanosized components for core-shell structure nanocomposite synthesis. In this case, the surface modification could be more facile. Compared with other kinds of porous materials, COFs can be applied as more suitable scaffolds for fabricating core-shell structured noble nanocomposite, based on the feasibly tuned properties by the in-built covalent bond architecture. Until now, a few transition metals immobilized in COF materials have been applied in different chemical reactions such as Suzuki coupling, Knoevenagel condensation, nitroarenes reduction, and so on [29]. However, COF-based transition metal catalysts have been seldom explored for the preparation of secondary amines. Generally speaking, the catalytic transformation of primary amides to the corresponding secondary imines requires expensive amines, and the primary amines are mostly obtained from the reductive amination reactions of carbonyl compounds with NH_3. So, it would be an ideal, green, and promising choice for the the secondary imines to be obtained through the direct reductive amination of aromatic aldehyde via a one-pot tandem process. Herein, a facile synthesis strategy of a Pd nanoparticles-anchored COF matrix was developed (Scheme 1d). We also evaluated its catalytic activity in the one-pot tandem reductive amination of benzaldehyde to amines. This system requires NH_3 as the nitrogen source and H_2 gas as the source of hydrogen. This process offered not only an atom-economical and environmentally friendly process for synthesizing amines but also minimized the workup and purification steps. What is more, this Pd/COF catalyst is also applicable for more than 20 aromatic, heterocyclic and cyclic aldehydes, and tolerates the presence of various functional groups with ortho-, meta-, and para-position substitutes under mild conditions (70 °C, 2 h, 20 bar of H_2).

2. Results and Discussion

2.1. Characterization of COF Support and Reduced COF-Supported Pd Catalyst

As shown in Figure 1a, for both **SJ02** and reduced COF-supported **Pd-SJ04** FTIR spectra (Figure S4), the peaks at 1573 cm^{-1} (-C=N bond) in the COF support **SJ02** and 1569 cm^{-1} (-C=N bond) in reduced COF-supported **Pd-SJ04** catalyst could be detected, which confirmed the formation of a Schiff base in the COF synthesis and the COF-supported catalyst. The peaks around 1251 and 1573 cm^{-1} can be assigned to C–N and typical C=C stretching vibration, respectively. Powder X-ray diffraction (PXRD) was performed to obtain the insight crystalline structure of the COFs. Figure 1b shows the PXRD analysis of the spherical COFs **SJ02** and reduced COF-supported **Pd-SJ04 (Figure S5)**. It is shown that the signals of reduced COF-supported **Pd-SJ04** show no significant changes in comparison to the COF support **SJ02**, indicating that the palladium salt introduction does not damage the overall crystallinity and retains the framework integrity of isolated COFs **SJ02**. Additionally, as shown in the reduced COF-supported **Pd-SJ04** catalyst, the peak at 6.4° is derived from COF support **SJ02** originally, and the relatively wide signal at around 26.3° agrees well with the (001) reflection. This phenomenon was ascribed to the $\pi-\pi$ stacking between the ordered adjacent layers of the COF sheets [30].

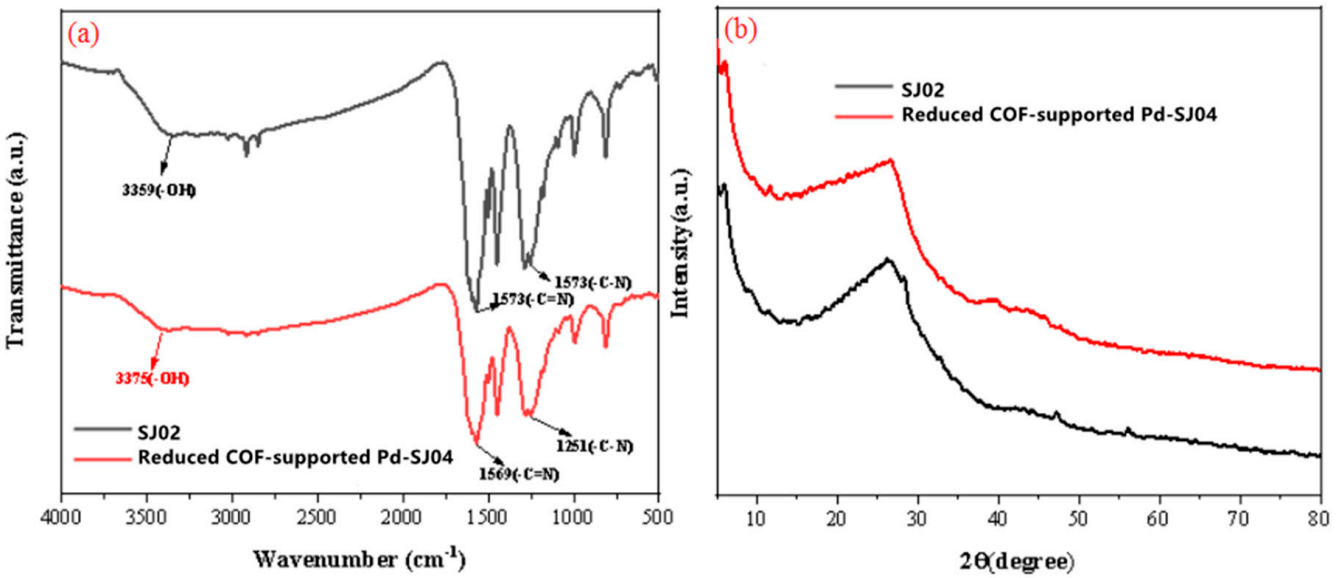


Figure 1. FTIR spectra (**a**) and XRD patterns (**b**) of **SJ02** and reduced COF-supported **Pd-SJ04.**

At the same time, as illustrated in Figure 2 (Figures S1,S2,S7, Table S3), reduced COF-supported **Pd-SJ04** exhibits an irregular morphology with an average size of about 100 nm. Furthermore, the elements of reduced COF-supported **Pd-SJ04** were further analyzed by the EDS mapping images. As depicted in Figure 2, other than C, N, and O, the Pd element is observed, suggesting that the Pd species is uniformly incorporated into the COF support **SJ02** matrix.

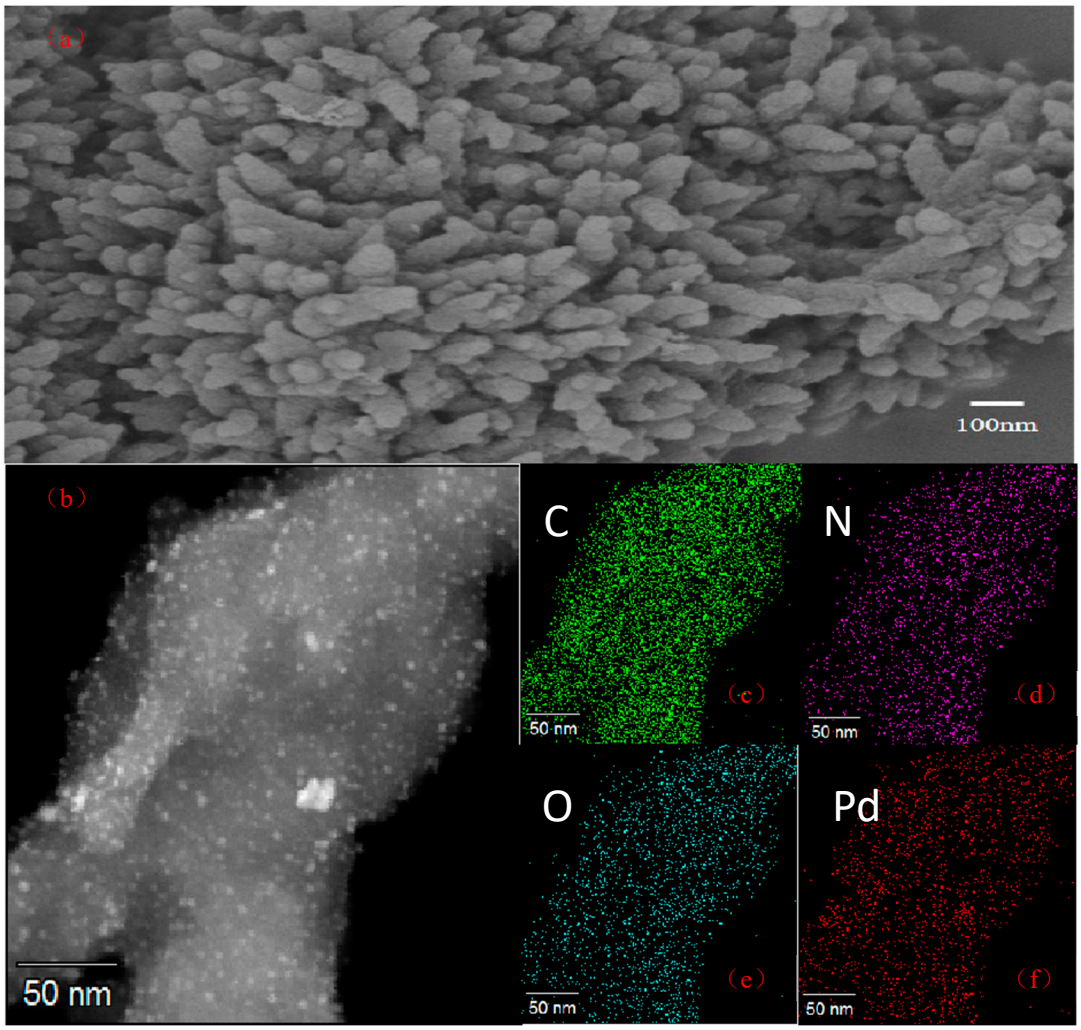


Figure 2. SEM image (**a**) and EDS mapping (**b–f**) of reduced COF-supported **Pd-SJ04.**

Nitrogen adsorption/desorption isotherms of the **SJ02** and reduced COF-supported **Pd-SJ04** are also displayed in Figure 3 (Figure S6, Table S2). Both the COF support and reduced COF-supported **Pd-SJ04** catalyst samples showed a type IV reversible adsorption isotherm curve, indicating the existence of mesopores. The Brunaue–Emmett–Teller surface area of **SJ02** and reduced COF-supported **Pd-SJ04** are calculated to be 559.531 and 347.076 $m^2 \cdot g^{-1}$, respectively. The V_{pore} of **SJ02** and reduced COF-supported **Pd-SJ04** dropped from 0.322 $cm^3\ g^{-1}$ to 0.254 $cm^3\ g^{-1}$ when incroporating of Pd in the framework, which could be ascribed to the fact that the Pd nanoparticles filled in the original pores of the COF matix. As shown in Figure 3b, based on the quenched solid density functional theory (QSDFT) model, the pore size distribution of both two samples revealed main peaks in the range of approximately 8 to 60 nm. In comparison with **SJ02**, the large decrease in the surface area and little change in the pore size distribution for reduced COF-supported **Pd-SJ04**, indicating that the presence of Pd species would not block the cavities of reduced COF-supported **Pd-SJ04** but could enhance the weight significantly. This pore distribution behavior and specific surface area might make COF-supported Pd materials to be tempting options for potential catalysis applications.

As shown in Figure 4, the XPS spectra of the COF support **SJ02** and reduced COF-supported **Pd-SJ04** catalyst were presented to further investigate surface structures and chemical states (Figure S3). The binding energies were corrected for specimen charging using C1s as the reference at 284.8 eV in the XPS analysis. It is clear to see the signals of Pd3d, N1s, C1s, and O1s in the reduced COF-supported **Pd-SJ04** catalyst, and the

signals of N1s, C1s, and O1s in the **SJ02** support. The corresponding high-resolution C 1s spectrum in Figure 4a shows two peaks at 284.8 and 285.1 eV, which matched with sp^3-coordinated hybridized carbons and C–N bond. Furthermore, the N1s spectrums of COF support **SJ02** and reduced COF-supported **Pd-SJ04** catalyst can be fitted into two peaks, which belonging to sp^2 hybridized nitrogen in the form of C-N=C and the C-N bond, respectively. C=O peak at 532.4 eV can be observed in the peak-fitted O 1s XPS spectra of COF support **SJ02** and reduced COF-supported **Pd-SJ04** catalyst. According to the high-resolution Pd3d XPS spectrum of reduced COF-supported **Pd-SJ04** catalyst, the $Pd3d^{5/2}$ was fitted into states at bonding energies of 335.8 eV and 338.4 eV, which can be ascribed to the presence of metal Pd^0 and Pd^{2+} species, respectively. Moreover, the $Pd3d^{3/2}$ was also fitted into states at bonding energies of 341.6 eV and 343.8 eV, and these were ascribed to the presence of metal Pd^0 and Pd^{2+} species, respectively. As is well known, Pd^0, like Pd/C, has a specific dissociation power for hydrogenation reaction; thus, the presence of $Pd^{\sigma+}$ could affect catalytic hydrogenolysis activity and further contribute to suppressing the over-hydrogenation reaction.

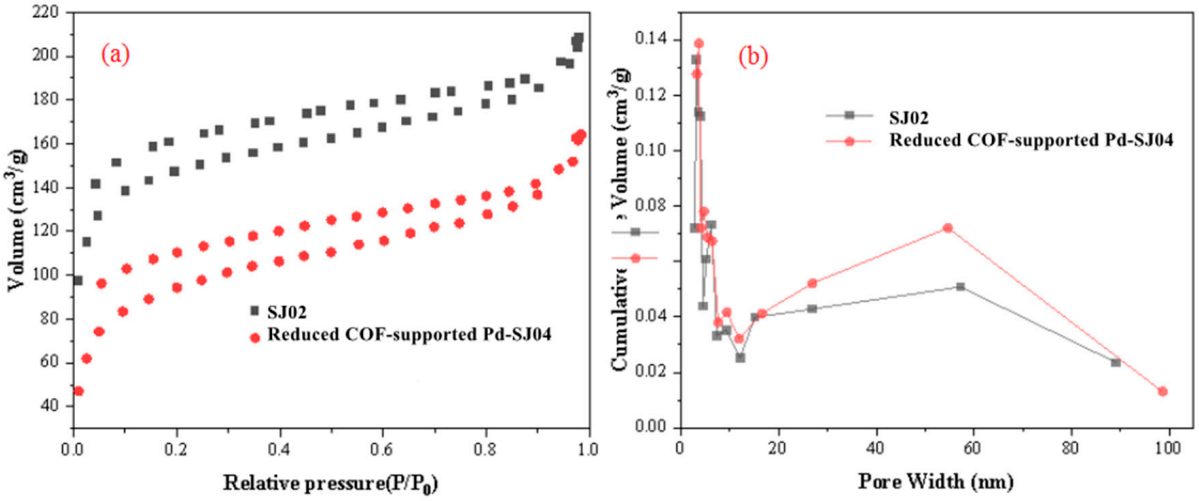


Figure 3. (**a**) Nitrogen adsorption–desorption isotherms and (**b**) pore size distribution of **SJ02** and reduced COF-supported **Pd-SJ04.**

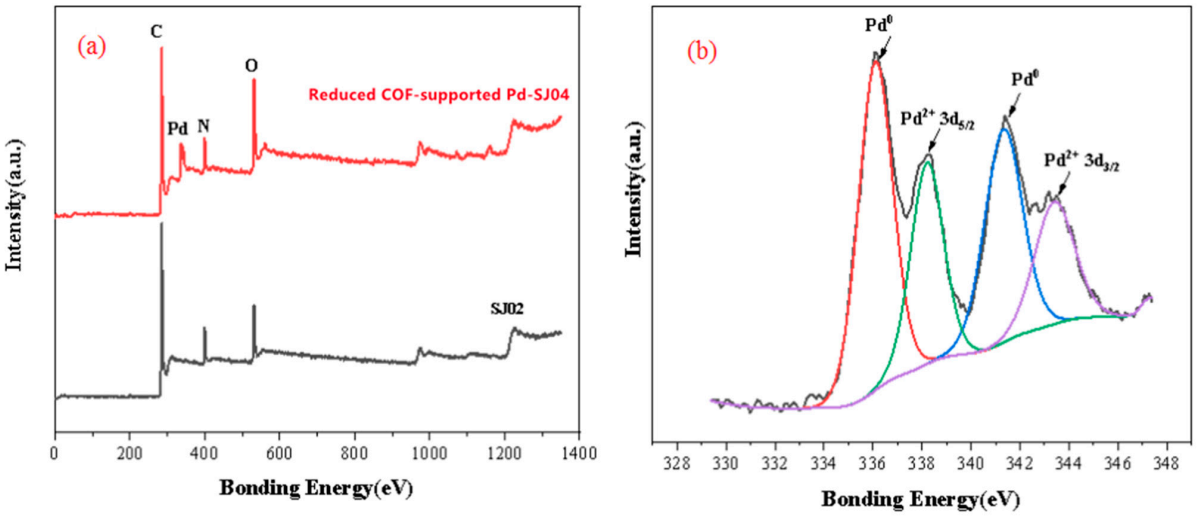
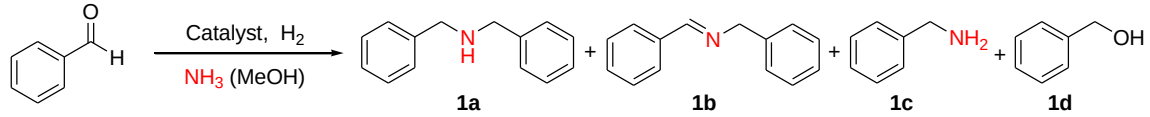


Figure 4. (**a**)The survey and (**b**) Pd3d high-resolution XPS spectra corresponding to reduced COF-supported **Pd-SJ04**. The survey spectrum of **SJ02** is also included as a reference sample.

2.2. Reduced COF-Supported Pd Catalyst Reductive Amination

With the ideal heterogeneous COF supported reduced COF-supported **Pd-SJ04** catalyst in hand, we investigated its catalytic activity for the direct reductive amination of benzaldehyde using NH_3. Generally speaking, H_2 pressure is a key factor, which can influence the reaction selectivity for the reductive reaction. As shown in Table 1 (Figure S9,S10), in this case, when the hydrogen pressure increased from 10 to 30 bar, the yield of dibenzylamine did not change dramatically and remained at about 80%. The reaction temperature had a great effect on the product distribution. When the reaction temperature was varied from 50, 70, 90, to 110 °C under 20 bar of hydrogen pressure, the yield of dibenzylamine increased first to 85.1% and then dropped to 72%. When the reaction was carried out over a long period of time from 2 to 12 h, this was not good for the selectivity of dibenzylamine; the product yield dropped from 83.8 to 72.3%.

Table 1. Optimizing the conditions for the reductive amination of benzaldehyde to dibenzylamine [a].



Catalyst: Reduced COF-supported **Pd-SJ04**

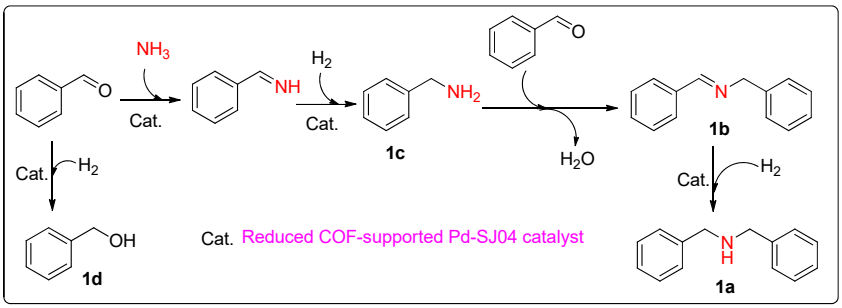
Entry	H_2 Pressure (bar)	Temperature (°C)	Time (h)	Conversion (%)	Yield of 1a (%)
1	10	90	4	>99	79.1
2	20	90	4	>99	81.7
3	30	90	4	>99	78.5
4	20	50	4	>99	75.6
5	20	70	4	>99	85.1
6	20	90	4	>99	81.7
7	20	110	4	>99	72.0
8	20	90	2	>99	83.8
9	20	90	4	>99	81.7
10	20	90	8	>99	76.9
11	20	90	12	>99	72.3
12	20	70	2	>99	87.6

[a] Reaction conditions: 5 mg catalyst, 0.5 mmol benzaldehyde, 5 mL Methanol ammonia solution. Yields and conversion were determined by NMR using 1, 3, 5-trimethoxybenzenen as an internal standard.

With the optimized reaction conditions in hand, we tested its great potential practical applicability for the reductive amination of the aldehyde with various functional substituted groups. As listed in Table 2, many different functional aromatic, heterocyclic, and cyclic aldehydes were well-tolerated under the optimized mild reaction conditions (70 °C, 2 h, 20 bar of H_2), which demonstrated its general applications in the field of reductive amination of aldehydes to target secondary imines (Figures S11–S33). For the para-substituted aromatic aldehydes, when the substituent group changed from methyl, methoxyl, chloro, fluoro to amine, the reductive amination provided the desired product in good to excellent selectivity (**3a** to **7a**). However, the substrates having amide, nitrile, and ethoxyl on the para-position were not well tolerated in this reaction condition (**8a**, **9a, 10a**). Generally speaking, the position of the aromatic substrates in the substituted group influenced its catalytic reactivity and product selectivity. As it shown in Table 2, benzaldehydes with meta-Cl, meta-OMe, and meta-F substituent group had much higher selectivity (**11a**: 66%; **13a**: 75%; **14a**: 67%) for corresponding amine than those in the ortho-position (**17a**: 43%; **18a**: 35%; **20a**: 53%). This phenomenon could be ascribed to the synergy of electronic nature and steric effects. To our excitement, the biomass platform compounds can be converted to their corresponding amines in excellent activity and good desired product selectivity (**21a**: 70%; **22a**: 65%). The aliphatic substrate aldehydes with either linear aldehydes or branched-chain aldehyde seemed to have substantial difficulty realizing the one-pot reductive amination and gave the desired product **24a** in 29% selec-

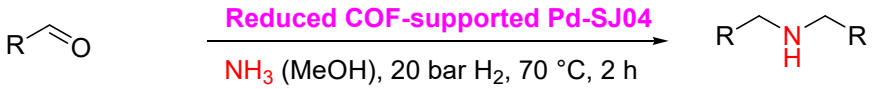
tivity, **25a** in 16% selectivity, **26a** in 40% selectivity, and **27a** in 19% selectivity, respectively. The cyclic aldehyde **23**, instead, can tolerate well and provided the desired amine product in full conversion and 67% selectivity. In conclusion, the heterogeneous COF-supported reduced COF-supported **Pd-SJ04** catalyst showed promising potential results for the one-pot reductive amination of aromatic, aliphatic, and heterocyclic aldehydes with various functional groups substituted, and many corresponding amines products were obtained in good to excellent selectivity under mild reaction conditions (70 °C, 2 h, NH_3, 20 bar H_2).

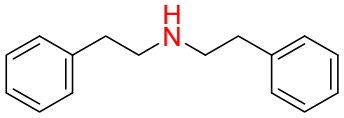
A possible catalytic reaction pathway for the benzaldehyde to dibenzylamine with NH_3 and H_2 gas has been proposed according to the results from the one-pot reductive amination of benzaldehyde and compared with the previously reported literature. As depicted in Scheme 2, the starting material benzaldehyde was firstly reacted with one molecule of ammonia and dehydrated to form the reactive intermediates benzylimine under the reduced COF-supported **Pd-SJ04** catalyst. During the reaction process, we did not observe the benzylimine product since it is very reactive in the reaction and prone to hydrogenate rapidly to **1c**. As was reported in the previous literature [31], H_2 and NH_3 adsorb completely on the same active metal sites and affect the reductive amination process dramatically. Moreover, a variation of the ratio for Pd^{2+} and Pd^0 species based on the XPS characterization analysis could greatly affect the hydrogenation and amination process. It was no wonder that the Pd^0 species also facilitated the **1d** formation and **1a** formation. Since there is a competitive process between **1c** and **1d** formation, precise controlling of the active sites of Pd^{2+} and Pd^0 species and its responding reactivity for selective amination process as well as reductive amination to form **1c** and reductive hydrogenation to form **1d** is very important. In the meantime, the **1c** was further reacted with another molecule of benzaldehyde and dehydrated to yield **1b** over reduced COF-supported **Pd-SJ04** catalyst. Then, the **1b** was further hydrogenated to the desired product **1a** using the reduced COF-supported **Pd-SJ04** catalyst, mainly relying on the Pd^0 species under H_2. All in all, this indicated that a suitable amount of NH_3, H_2, and the precise regulation of Pd^{2+} and Pd^0 species for the reduced COF-supported **Pd-SJ04** catalyst, were of great significance for the high selectively transformation and efficiency conversion to the desired product, dibenzylimine.



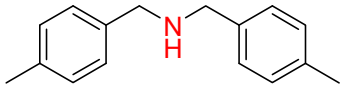
Scheme 2. Proposed reaction pathways for the reductive amination of benzaldehyde over the reduced COF-supported **Pd-SJ04** catalyst.

Table 2. Screening of aldehydes to synthesize dibenzylamine homologs.

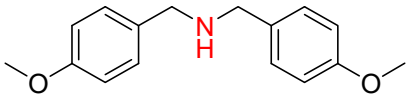




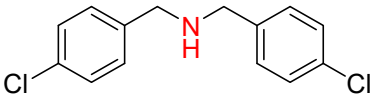
2a:full con,75% sel



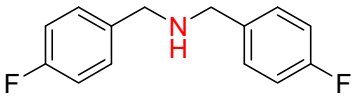
3a: full con,88% sel



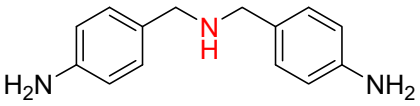
4a: full con,91% sel



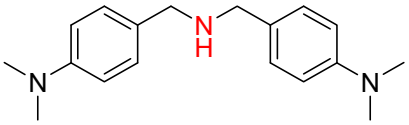
5a:full con,65% sel



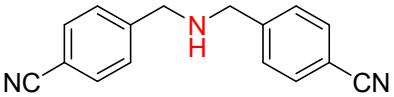
6a:full con,90% sel



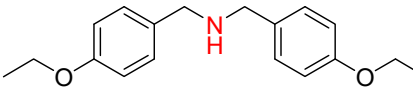
7a: full con,79% sel



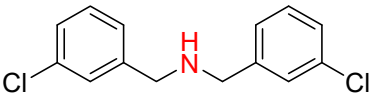
8a: full con,34% sel



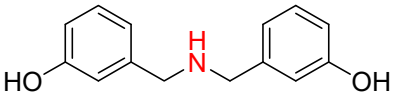
9a: full con,17% sel



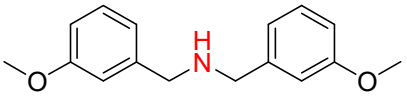
10a: full con,34% sel



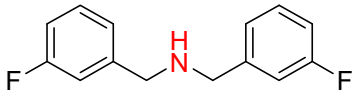
11a:full con,66% sel



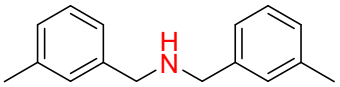
12a: full con,72% sel



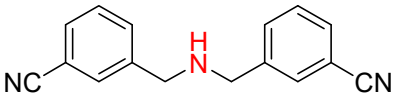
13a: full con,75% sel



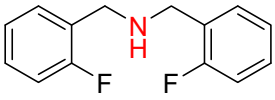
14a:full con,67% sel



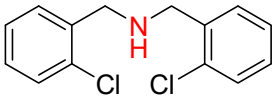
15a:full con,49% sel



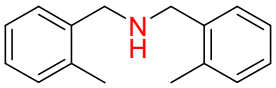
16a:full con,32% sel



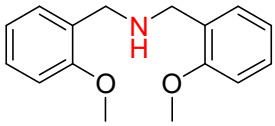
17a: full con,43% sel



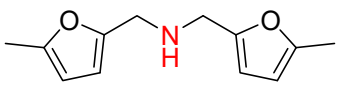
18a: full con,35% sel



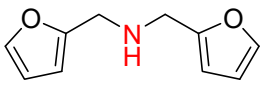
19a: full con,65% sel



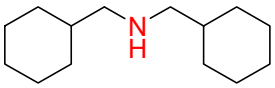
20a: full con,53% sel



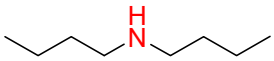
21a:98% con,70% sel



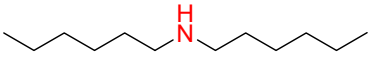
22a: full con,65% sel



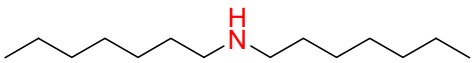
23a: full con,67% sel



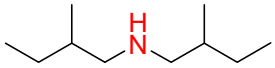
24a: full con,29% sel



25a: full con,16% sel



26a: full con,40% sel



27a: full con,19% sel

Reaction conditions: 5 mg catalyst, 0.5 mmol aldehydes, 5 mL Methanol ammonia solution. Yields and conversions were determined by GC with the internal standard.

3. Materials and Methods

3.1. Chemicals and Materials

The aldehyde starting material and the chemical reagents were used without purification. The solvent EtOH (AR, water ≤0.3%), DMF (Biotechnology grade, ≥99.9%), CH_2Cl_2 (Standard for GC, ≥ 99.7%, 50–150 ppm Isoamylene stabilizer), MeOH (≥99.9% (GC)) used in this work were purchased from Shanghai Aladdin Bio-Chem Technology Co., Ltd. (Shanghai, China). and used directly. The 1,3,5 trimethoxybenzene (99%) was bought from the Alfa Aesar Chemical Co., Ltd. (Shanghai, China); the Ammonia solution (2.0 mol/L in MeOH) was purchased from the Energy-chemical Co., Ltd. (Shanghai, China); Citric acid (AR, ≥ 99.5%), $CDCl_3$ (99.8% D, stabilized with Ag, containing 0.03% TMS), 1, 4 dioxanes (AR, 99% containing 10 ppm BHT as a stabilizer), tetrahydrofuran (99.5%, with molecular sieves, Water ≤ 50 ppm, stabilized with BHT) and acetate (AR, 99.5%) were obtained from Shanghai Macklin Biochemical Co., Ltd. (Shanghai, China). N and N-Dimethylformamide (AR ≥ 99.5%) were purchased from Guangzhou Chemical Reagent Factory (Guangzhou, China). $Pd(OAc)_2$ (AR, > 98.0%) was bought from TCI (Shanghai) Chemical Industry Development Co., Ltd. (Shanghai, China). Sodium borohydride (AR, >98.0%) was purchased from Tianjin Damao Chemical Reagent Factory (Tianjin, China).

3.2. Catalyst Preparation

3.2.1. Synthesis of COF Material

The spherical COF material was synthesized via the previously reported facile hydrothermal method [32]. The COF material was synthesized by reacting 2, 4, 6-Trihydroxybenzene-1, 3, 5-tricarbaldehyde (200 mg, 0.92 mmol) with 6-(5-aminopyridin-2-yl)pyridin-3-amine (215.2 mg, 1.11 mmol) for 1 h in the presence of anhydrous EtOH (60 mL) at room temperature. The crude reaction products were collected and dispersed into DMF at 153 °C to 160 °C for 4 h. After filtration, the collecting powder was then immersed in anhydrous EtOH at 80 °C for 2 h. Finally, the powder was dried under vacuum conditions at 80 °C for 24 h. The resulting COF material was named SJX. In brief, the 2, 4, 6-Trihydroxy-benzene-1, 3, 5-tricarbaldehyde was served as a monomer, reacting with 6-(5-aminopyridin-2-yl)pyridin-3-amine via Schiff's base reaction, and then denoted as **SJ02**.

3.2.2. Synthesis of COF Based Pd Catalyst

Pre-synthesized COF support material **SJ02** (165 mg) was put in 10 to 20 mL of dichloromethane, and palladium acetate (20 mg, 0.089 mmol) was added. This reaction mixture was stirred at room temperature for 24 h. We then recovered the residue by filtration and washed with DCM in a Soxhlet extractor for 24 h. Finally, the sample **Pd-SJ04** was dried under vacuum conditions at 80 °C.

3.2.3. Synthesis of the Reduced COF-Supported Pd Catalyst

The Pd ions were subsequently introduced into COFs, and the strong coordination was built between Pd metal ions and nitrogen atoms in the COF matrix. The COF-based Pd catalyst **Pd-SJ04** (148 mg) and sodium borohydride (3.97 mg, 1.5 times the molar amount of Pd) were stirred in methanol solution for 24 h. Finally, the reduced COF-supported Pd catalyst **Pd-SJ04** was further dried at 90 °C for 12 h under vacuum conditions. The metal Pd particles were stably anchored on COF support after the reduction process by $NaBH_4$.

3.3. Catalyst Characterization

Powder X-ray diffraction (XRD) patterns were recorded by an X' Pert Pro system, using Cu-Kα radiation with a $\Delta 2\theta = 0.02^\circ$ in the 2.5° to 50° 2θ range (X'Pert PRO MPD, PANalytical, Netherlands). X-ray photoelectron spectroscopy (XPS) was recorded with an AXIS Ultra DLD (Kratos, Britain) and the standard C 1s peak was used as a reference for correcting the shifts. Field-emission scanning electron microscope (FESEM) images were acquired on a JEOL JSM-6700 electron microscope (JEOL, Japan). Fourier Transform infrared spectroscopy (FTIR) was mainly used for group structure analysis of materials,

qualitative and quantitative analysis of materials, especially qualitative analysis of the functional group characteristic absorption frequency. IR spectra were recorded on a Bruker Tensor 27 spectrometer with dried KBr (Berlin, Germany). The N_2 adsorption-desorption isotherms were measured with a Tristar 3010 isothermal nitrogen sorption analyzer (Micromeritics, Florida, USA) at 77 K after the samples were degassed in a vacuum at 120 °C for 10 h.

3.4. General Procedure for the Catalytic Reductive Amination Reaction

The reductive amination of aldehydes was carried out in a stainless-steel autoclave reactor (Anhui Kemi Machinery Technology Co., LTD, China) with six channels. In a standard run for the catalytic activity test of this reduced COF-supported Pd catalyst **Pd-SJ04**, aldehyde substance (0.5 mmol), reduced COF-supported **Pd-SJ04** catalyst (5 mg), and 5 mL 2.0 mol/L ethanol solution of ammonia were added into the reactor with a Teflon coated stir bar. The reactor was sealed and then purged three times with hydrogen, followed by filling with H_2 to 1–3 MPa and heating to the target temperature of 50 to 110 °C and stirred vigorously for a settled time (2 to 12 h). We cooled down the reaction autoclave to room temperature and separated the catalyst by a 0.22-μm filtering membrane. The mixture was analyzed by ^{1}H NMR spectra spectroscopy or GC. The yield of the reaction was studied by the internal standard method (1, 3, 5 trimethoxybenzene as an internal standard).

4. Conclusions

In summary, we have designed and successfully synthesized the COF-supported material and the COF-supported heterogeneous reduced COF-supported **Pd-SJ04** catalyst. The latter showed high reactivity and selectivity of amines for the facile and efficient one-pot reductive amination from aldehydes for the first time. The Pd nanoparticles were anchored on the COF supports successfully. It was found that both the metallic state of Pd and oxidated $Pd^{\sigma+}$ existed in the catalysts based on the XPS analysis. In particular, the reduced COF-supported **Pd-SJ04** catalyst could catalyze many aromatic, aliphatic, and heterocyclic aldehydes with various functional groups substituted to their corresponding amines products in good to excellent selectivity under mild reaction conditions (70 °C, 2 h, NH_3, 20 bar H_2). This work makes the synthesis of secondary amine more economical and practical through the one-pot reductive amination process, since there are generally many undesired products, such as phenylmethanol, phenylmethanamine, and (E)-N-benzylidene-1-phenylmethanamine, occurring in the reductive amination of benzaldehyde. Moreover, further studies are in progress to design the more stable and precise regulation of Pd-based catalyst and investigate the detailed mechanism of COF-supported Pd catalyzed reductive amination.

Supplementary Materials: The following are available online at https://www.mdpi.com/2073-4344/11/2/287/s1, Figure S1: SEM images of Reduced COF-supported Pd-SJ04. Figure S2: TEM mapping of Reduced COF-supported Pd-SJ04. Figure S3: (a) The survey spectra and (b) high-resolution XPS spectra of Pd3d for Reduced COF-supported Pd-SJ04. Figure S4: The FTIR spectra of SJ-02 and Reduced COF-supported Pd-SJ04. Figure S5: XRD patterns of SJ-02 and Reduced COF-supported Pd-SJ04. Figure S6: (a) Nitrogen adsorption-desorption isotherms and (b) pore size distribution of SJ-02 and Reduced COF-supported Pd-SJ04. Table S1: Comparison with Other Reported Catalysts for the Hydrogenation of Alkynes. Figure S7: Elemental analysis of Reduced COF-supported Pd-SJ04. Table S2: Specific surface area, pore volume, pore diameter of SJ-02 and Reduced COF-supported Pd-SJ04. Table S3: The element contents of the as-prepared catalysts determined by TEM spectrum. Figure S8: ^{1}H NMR spectra of phenylacetylene. Figure S9: ^{1}H NMR spectra of diphenethylamine. Figure S10: GC-MS spectra of diphenethylamine. Figure S11: ^{1}H NMR spectra of bis(4-methylbenzyl)amine. Figure S12: GC-MS spectra of bis(4-methylbenzyl)amine. Figure S13: ^{1}H NMR spectra of N, N-bis(p-methoxybenzyl)amine. Figure S14: GC-MS spectras of N, N-bis(p-methoxybenzyl)amine. Figure S15: ^{1}H NMR spectras of bis((furan-2-yl)methyl)amine. Figure S16. GC-MS spectras of bis((furan-2-yl)methyl)amine. Figure S17: ^{1}H NMR spectras of 1-(4-fluorophenyl)-

N-[(4-fluorophenyl)methyl]methanamine. Figure S18: GC-MS spectras of 1-(4-fluorophenyl)-N-[(4-fluorophenyl)methyl]methanamine. Figure S19: ^{1}H NMR spectras of N, N-bis(4-chlorobenzyl)amine. Figure S20: GC-MS spectras of N, N-bis(4-chlorobenzyl)amine. Figure S21: ^{1}H NMR spectras of bis-(5-methyl-furan-2-ylmethyl)-amine. Figure S22: GC-MS spectras of bis-(5-methyl-furan-2-ylmethyl)-amine. Figure S23: ^{1}H NMR spectras of bis(2-methylbenzyl)amine. Figure S24: GC-MS spectras of bis(2-methylbenzyl)amine. Figure S25: ^{1}H NMR spectras of N, N-bis(m-methoxybenzyl)amine. Figure S26: GC-MS spectras of N, N-bis(m-methoxybenzyl)amine. Figure S27: ^{1}H NMR spectras of bis(3-fluorobenzyl)amine. Figure S28: GC-MS spectras of bis(3-fluorobenzyl)amine. Figure S29: ^{1}H NMR spectra of N, N-bis(3-chlorobenzyl)amine. Figure S30: GC-MS spectras of N, N-bis(3-chlorobenzyl)amine. Figure S31: ^{1}H NMR spectra of bis(4-aminobenzyl)amine. Figure S32: ^{1}H NMR spectra of N, N-bis(3-hydroxybenzyl)amine. Figure S33: GC-MS spectras of N, N-bis(3-hydroxybenzyl)amine.

Author Contributions: J.L. and L.M. conceived and designed the experiments. M.Z. performed experiments and prepared the Supplementary Information. J.L. wrote the paper. All authors discussed the results and commented on the manuscript. All authors have read and agreed to the published version of the manuscript.

Funding: This research was funded by [National Key R&D Program of China] grant number [2018YFB1501502], [National Natural Science Foundation of China] grant number [51976225], [Dalian National Laboratory Cooperation Foundation] grant number [DNL201916]. And The APC was funded by [National Natural Science Foundation of China] and [Dalian National Laboratory Cooperation Foundation].

Data Availability Statement: Data is contained within the article or supplementary material. The data presented in this study are available in [supplementary material of Facile Synthesis of COF-Supported Reduced Pd-based Catalyst for One-Pot Reductive Amination of Aldehydes].

Conflicts of Interest: The authors declare no competing interests.

References

1. Choucair, B.; Leon, H.; Mire, M.-A.; Lebreton, C.; Mosset, P. Indium- or zinc-mediated one-pot synthesis of homoallylamines, beta-amino esters, and beta-amino nitriles. *Org. Lett.* **2000**, *2*, 1851–1853. [CrossRef]
2. Harrington, P.E.; Jean, D.J.S., Jr.; Clarine, J.; Coulter, T.S.; Croghan, M.; Davenport, A.; Davis, J.; Ghiron, C.; Hutchinson, J.; Kelly, M.G.; et al. The discovery of an orally efficacious positive allosteric modulator of the calcium sensing receptor containing a dibenzylamine core. *Bioorg. Med. Chem. Lett.* **2010**, *20*, 5544–5547. [CrossRef]
3. Qi, F.; Hu, L.; Lu, S.; Cao, X.; Gu, H. Selective synthesis of secondary amines by Pt nanowire catalyzed reductive amination of aldehydes and ketones with ammonia. *Chem. Commun.* **2012**, *48*, 9631–9633. [CrossRef]
4. Jagadeesh, R.V.; Murugesan, K.; Alshammari, A.S.; Neumann, H.; Pohl, M.M.; Radnik, J.; Beller, M. MOF-derived cobalt nanoparticles catalyze a general synthesis of amines. *Science* **2017**, *358*, 326–332. [CrossRef]
5. Liang, G.; Wang, A.Q.; Li, L.; Xu, G.; Yan, N.; Zhang, T. Production of Primary Amines by Reductive Amination of Biomass-Derived Aldehydes/Ketones. *Angew. Chem. Int. Ed.* **2017**, *56*, 3050–3054. [CrossRef]
6. Lu, S.; Xu, P.; Cao, X.; Gu, H.W. A highly active worm-like PtMo nanowire for the selective synthesis of dibenzylamines. *RSC Adv.* **2018**, *8*, 8755–8760. [CrossRef]
7. Li, M.; Pischetola, C.; Cardenas-Lizana, F.; Keane, M.A. Production of benzylamine by tandem dehydrogenation/amination/reduction over Cu and Au catalysts. *Appl. Catal. A Gen.* **2020**, *590*, 117368. [CrossRef]
8. Salvatore, R.N.; Yoon, C.H.; Jung, K.W. Synthesis of secondary amines. *Tetrahedron* **2001**, *57*, 7785–7811. [CrossRef]
9. Kumar, R.; Gleissner, E.H.; Tiu, E.G.V.; Yamakoshi, Y. C-70 as a Photocatalyst for Oxidation of Secondary Benzylamines to Imines. *Org. Lett.* **2016**, *18*, 184–187. [CrossRef] [PubMed]
10. Li, H.F.; AI-Dakhil, A.; Lupp, D.; Gholap, S.S.; Lai, Z.P.; Liang, L.C.; Huang, K.W. Cobalt-Catalyzed Selective Hydrogenation of Nitriles to Secondary Imines. *Org. Lett.* **2018**, *20*, 6430–6435. [CrossRef]
11. Pagnoux-Ozherelyeva, A.; Pannetier, N.; Mbaye, M.D.; Gaillard, S.; Renaud, J.L. Knolker's Iron Complex: An Efficient In Situ Generated Catalyst for Reductive Amination of Alkyl Aldehydes and Amines. *Angew. Chem. Int. Ed.* **2012**, *51*, 4976–4980. [CrossRef] [PubMed]
12. Park, J.W.; Chung, Y.K. Hydrogen-Free Cobalt-Rhodium Heterobimetallic Nanoparticle-Catalyzed Reductive Amination of Aldehydes and Ketones with Amines and Nitroarenes in the Presence of Carbon Monoxide and Water. *ACS Catal.* **2015**, *5*, 4846–4850. [CrossRef]
13. Hahn, G.; Kunnas, P.; de Jonge, N.; Kempe, R. General synthesis of primary amines via reductive amination employing a reusable nickel catalyst. *Nat. Catal.* **2019**, *2*, 71–77. [CrossRef]

14. Murugesan, K.; Beller, M.; Jagadeesh, R.V. Reusable Nickel Nanoparticles-Catalyzed Reductive Amination for Selective Synthesis of Primary Amines. *Angew. Chem. Int. Ed.* **2019**, *58*, 5064–5068. [CrossRef] [PubMed]
15. Cuypers, T.; Morias, T.; Windels, S.; Marquez, C.; Vankelecom, I.; De Vos, D.E. Ni-Catalyzed reductive amination of phenols with ammonia or amines into cyclohexylamines. *Green Chem.* **2020**, *22*, 1884–1893. [CrossRef]
16. Murugesan, K.; Chandrashehar, V.G.; Senthamarai, T.; Jagadeesh, R.V.; Beller, M. Reductive amination using cobalt-based nanoparticles for synthesis of amines. *Nat. Protoc.* **2020**, *15*, 1313–1337. [CrossRef]
17. Zheng, J.X.; Roisnel, T.; Darcel, C.; Sortais, J.B. Nickel-Catalysed Reductive Amination with Hydrosilanes. *ChemSusChem* **2013**, *5*, 2861–2864. [CrossRef]
18. Tanabe, M.; Yumoto, R.; Osakada, K. Reaction of an alkyne with dinickel-diphenylsilyl complexes. An emissive disilane formed via the consecutive Si-C and Si-Si bond-making processes. *Chem. Commun.* **2012**, *48*, 2125–2127. [CrossRef] [PubMed]
19. Xie, J.H.; Zhu, S.F.; Zhou, Q.L. Transition Metal-Catalyzed Enantioselective Hydrogenation of Enamines and Imines. *Chem. Rev.* **2011**, *111*, 1713–1760. [CrossRef]
20. Grirrane, A.; Garcia, H.; Corma, A. Supported palladium nanoparticles as heterogeneous ligand-free catalysts for the Hiyama C-C coupling of vinylsilanes and halobenzenes leading to styrenes. *J. Catal.* **2013**, *302*, 49–57. [CrossRef]
21. Wang, Y.F.; Xiao, Z.M.; Wu, L. Metal-nanoparticles Supported on Solid as Heterogeneous Catalysts. *Curr. Org. Chem.* **2013**, *17*, 1325–1333. [CrossRef]
22. Navalon, S.; Dhakshinamoorthy, A.; Alvaro, M.; Garcia, H. Metal nanoparticles supported on two-dimensional graphenes as heterogeneous catalysts. *Coord. Chem. Rev.* **2016**, *312*, 99–148. [CrossRef]
23. Sankar, M.; He, Q.; Engel, R.V.; Sainna, M.A.; Logsdail, A.J.; Roldan, A.; Willock, D.J.; Agarwal, N.; Kiely, C.J.; Hutchings, G.J. Role of the Support in Gold-Containing Nanoparticles as Heterogeneous Catalysts. *Chem. Rev.* **2020**, *120*, 3890–3938. [CrossRef]
24. Cote, A.P.; Benin, A.I.; Ockwig, N.W.; O'Keeffe, M.; Matzger, A.J.; Yaghi, O.M. Porous, crystalline, covalent organic frameworks. *Science* **2005**, *310*, 1166–1170. [CrossRef]
25. Xu, H.; Gao, J.; Jiang, D.L. Stable, crystalline, porous, covalent organic frameworks as a platform for chiral organocatalysts. *Nat. Chem.* **2015**, *7*, 905–912. [CrossRef]
26. Huang, N.; Zhai, L.P.; Coupry, D.E.; Addicoat, M.A.; Okushita, K.; Nishimura, K.; Heine, T.; Jiang, D.L. Multiple-component covalent organic frameworks. *Nat. Commun.* **2016**, *7*, 12325. [CrossRef]
27. Yoo, J.; Cho, S.J.; Jung, G.Y.; Kim, S.H.; Choi, K.H.; Kim, J.H.; Lee, C.K.; Kwak, S.K.; Lee, S.Y. COF-Net on CNT-Net as a Molecularly Designed, Hierarchical Porous Chemical Trap for Polysulfides in Lithium-Sulfur Batteries. *Nano Lett.* **2016**, *16*, 3292–3300. [CrossRef]
28. Li, Y.; Yang, C.X.; Yan, X.P. Controllable preparation of core-shell magnetic covalent-organic framework nanospheres for efficient adsorption and removal of bisphenols in aqueous solution. *Chem. Commun.* **2017**, *53*, 2511–2514. [CrossRef]
29. Liu, J.G.; Wang, N.; Ma, L.L. Recent Advances in Covalent Organic Frameworks for Catalysis. *Chem. Asian J.* **2020**, *15*, 338–351. [CrossRef] [PubMed]
30. Bhadra, M.; Sasmal, H.S.; Basu, A.; Midya, S.P.; Kandambeth, S.; Pachfule, P.; Balaraman, E.; Banerjee, R. Predesigned Metal-Anchored Building Block for in Situ Generation of Pd Nanoparticles in Porous Covalent Organic Framework: Application in Heterogeneous Tandem Catalysis. *ACS Appl. Mater. Interfaces* **2017**, *9*, 13785–13792. [CrossRef]
31. Fiore, A.M.; Romanazzi, G.; Dell'Anna, M.M.; Latronico, M.; Leonelli, C.; Mali, M.; Rizzuti, A.; Mastrorilli, P. Mild and efficient synthesis of secondary aromatic amines by one-pot stepwise reductive amination of arylaldehydes with nitroarenes promoted by reusable nickel nanoparticles. *Mol. Catal.* **2019**, *476*, 110507. [CrossRef]
32. Liu, J.G.; Wang, N.; Liu, J.N.; Li, M.; Xu, Y.; Wang, C.G.; Wang, Y.Z.; Zheng, H.Q.; Ma, L.L. The Immobilization of Pd(II) on Porous Organic Polymers for Semihydrogenation of Terminal Alkynes. *ACS Appl. Mater. Interfaces* **2020**, *12*, 51428–51436. [CrossRef] [PubMed]